Direct Observation of Surface Alloying and Interface Roughening: Growth of Au on Fe(001)

M. M. J. Bischoff, T. Yamada, A. J. Quinn,* R. G. P. van der Kraan,[†] and H. van Kempen[‡]

Research Institute for Materials, University of Nijmegen, 6525 ED Nijmegen, The Netherlands
(Received 11 July 2001; published 21 November 2001)

Scanning tunneling microscopy studies on the growth of Au on Fe(001) are reported. A surface alloy is observed for submonolayer deposition (<0.5 monolayer) at temperatures higher than 370 K. This surface-confined alloy demixes when it is covered with Au and in combination with imperfect layer-by-layer growth a rough interface consisting of Au islands *in* and Fe islands *on* the original Fe(001) substrate is created. A real-space high resolution study of this buried interface is possible because of the large difference in interlayer spacing between bcc Fe(001) and fcc Au(001).

Interfaces play a key role in the transport and magnetic properties of multilayer systems which are of technological and fundamental interest. Effects such as giant magnetoresistance [1], tunnel magnetoresistance [2], and oscillatory exchange coupling [3] display extreme sensitivity to interfacial conditions. Intermixing and interface roughening are important processes which strongly influence the interface quality.

During the last decade, the scanning tunneling microscope (STM) has proven to be a very useful tool in studying surface alloying. Chemical contrast has often been achieved either with special tip conditions (see, e.g., [4] and references therein) or by means of characteristic features in scanning tunneling spectroscopy (STS) [5]. However, reports on imaging of structures buried under metallic overlayers (i.e., a buried interface) are rare [6–8].

The large difference in interlayer spacing between bcc Fe(001) and fcc Au(001) (0.144 and 0.204 nm, respectively) makes this system ideal for a high resolution STM study of the subsurface interface. Their close lateral match (only 0.6% difference) is very favorable and, consequently, growth of Fe on Au(001) has been studied extensively (e.g., [9–11]). Despite the unfavorable surface energy relation ($\gamma_{Au} \ll \gamma_{Fe}$) layer-by-layer growth was often found and seems promoted by a surfactant Au monolayer floating on top of the Fe layer. Nevertheless, Blum *et al.* recently concluded that the growth of a flat and defect-free bcc-Fe film on Au(001) remains a challenge [10]. In contrast, the growth of Au on Fe(001) is not as widely studied. RHEED studies by Unguris *et al.* indicated that at 373 K the growth of Au on Fe(001) is well ordered and layer by layer [12]. However, the exchange coupling strength for a Fe/Au/Fe trilayer was found to be much lower than predicted by theory, in spite of the high quality of the Fe(001) whisker substrates used [3]. Recently, Opitz *et al.* postulated that the origin of this discrepancy is due to impurity scattering (i.e., intermixing of Au and Fe) at the interface rather than mesoscopic roughness [13].

In this Letter we show that in spite of the immiscibility of Au in bulk Fe a surface alloy is found for submonolayer deposition of Au on Fe(001) at temperatures higher than 370 K. For coverages larger than 0.5 monolayer the surface-confined alloy demixes and in combination with nonideal layer-by-layer growth behavior, a rough interface is obtained which comprises Au islands *in* and Fe islands *on* the original atomically flat Fe(001) substrate layer. A real-space high resolution STM study on this buried interface is presented.

The STM experiments were performed in ultrahigh vacuum using an Omicron UHV STM-1. Electrochemically etched W tips were cleaned and sharpened *in situ* by Ne self-sputtering [14]. A single crystal Fe(001) whisker was used as the substrate which was cleaned by cycles of Ar ion sputtering around 1000 K followed by radiative cooling to room temperature, which was sufficient to repair any surface damage (terraces >200 nm wide can be observed in STM). The concentration of surface impurities (mainly oxygen) was mostly below 1% as estimated from Auger electron spectroscopy and atomically resolved STM images. Gold (99.99% pure) was evaporated (rate of 0.2 monolayer/min as determined by a quartz crystal microbalance) from a Knudsen cell inside a liquid nitrogen cryoshroud to keep the pressure below 3×10^{-10} mbar during growth. One monolayer (ML) is defined as the amount of atoms in one Fe(001) layer. The sample temperature was measured by a thermocouple mounted close to (but not in direct contact with) the sample making the temperature measurements quite inaccurate (± 30 K).

An STM image of the Fe(001) surface after deposition of 0.20 ML Au at 400 K is shown in Fig. 1(a) and reveals islands, depressions, and protrusions. The terrace depressions (marked D; 30 pm deep and 7% concentration) are also visible on the uncovered Fe(001) surface and are related to oxygen contaminants. [Note that the contamination in this image is slightly higher compared to the following images, which was related to an improper cleaning of the Fe(001) whisker.] The small protrusions (marked P; 10% concentration) are visible only after Au deposition at temperatures higher than 400 K with increasing concentrations for increasing deposition temperatures. Because of their spherical symmetry (0.4 nm wide), low apparent height [10–20 pm; see Fig. 1(a) inset] and extreme sensitivity of their appearance on the tip conditions these features are identified as single substitutional Au
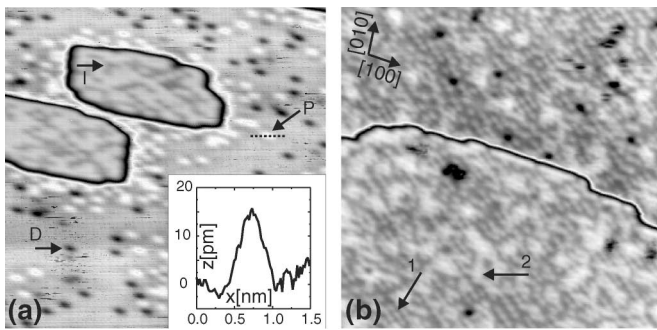
FIG. 1.   (a) STM image of 0.20 ML Au deposited on Fe(001) at 400 K (10×10 nm^2, $V_s = -0.77$ V, $I = 0.23$ nA). In addition to the depressions (e.g., arrow marked D, protrusions (P) are observed on the terrace, while on the islands only depressions (I) are observed. The inset shows a cross section along the dashed black line over protrusion P. (b) STM image of 0.44 ML Au deposited at 500 K (14.6×14.6 nm^2, $V_s = -0.07$ V, $I = 0.52$ nA). The terrace and the island (bottom) have the same composition for growth at this temperature. The close-packed directions of the Fe(001) lattice have been copied from Fig. 2. The arrows marked 1 and 2 indicate a local $c(2 \times 2)$ ordered area and a bright line parallel to the [010] direction, respectively. In both images the grey scale used is stepped: the black-white range corresponds to 0.05 nm on the terrace and on the island surface. The black (white) island perimeters are grey scale artifacts. The heights of the islands equal the Fe(001) step height (0.14 nm) within the accuracy of the measurement. All images presented in this Letter are raw data and have not been corrected for drift which explains the nonorthogonal appearance of the lattice directions.

atoms in the Fe(001) surface layer. Analogously, the weak depressions visible on the islands (marked I, 10–20 pm deep) are interpreted as place exchanged Fe atoms which have formed islands with Au adatoms. This interpretation is in agreement with the fact that 40% of the surface of the islands is covered with depressions. Since the islands cover 0.20 ML of the Fe(001) substrate (which equals the amount of Au deposited and shows that the number of Au atoms attached to step edges can be neglected for large terrace whisker substrates), it follows that 0.08 ML Fe can be found in the islands. Consequently, 0.08 ML Au is substituted in the Fe(001) terrace which perfectly agrees with the concentration observed. This balance and results obtained at slightly different growth temperatures and coverages also show that the Au atoms stay in the surface layer.

Upon deposition of 0.44 ML Au at 500 K a homogeneous surface layer is formed [Fig. 1(b)]. Protrusions are now visible on both the terrace and the island layers. Although the protrusions order locally in a $c(2 \times 2)$ structure (arrow 1) or even in clusters along close-packed directions (arrow 2), long-range order was not observed. Postannealing this sample to 650 K did not generate long-range order. STS shows that the Fe(001) surface state (see, e.g., [15]) has disappeared on this surface; instead a peak is observed around 0.6–0.7 eV above the Fermi level (see Bischoff [21]) on both terrace and islands giving another indication for the equal character of terrace and islands.
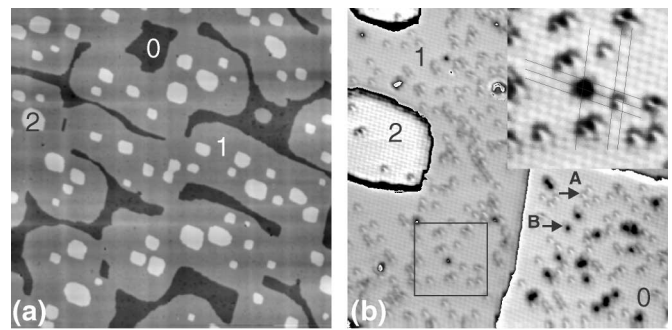
FIG. 2.   (a) STM image of 0.96 ML Au deposited on Fe(001) at 500 K (100×100 nm^2, $V_s = 1.0$ V, $I = 0.07$ nA). The growth mode is not perfectly layer by layer at this temperature: 0.15 ML of the original substrate (marked 0) is still uncovered, while already 0.11 ML of the first deposited layer (marked 1) is covered by islands (marked 2). All step heights in this image are 0.14 nm. (b) Higher resolution image of the same sample as (a). (20×20 nm^2, $V_s = -0.58$ V, $I = 0.25$ nA). A stepped grey scale has been used (numbers in image refer to level). On the $p(1 \times 1)$ lattice, asymmetric protrusions (marked A) and circular depressions (marked B) are observed which are ascribed to intermixed Fe atoms and contaminants, respectively. The inset shows the boxed area. The depression is centered at a fourfold hollow site, while the asymmetric feature comprises two unit cell depressions separated by a protrusion at a bridge site. These (highly tip dependent) appearances of the Fe atoms are ascribed to nontrivial tip-sample interactions leading to chemical contrast.

The formation of a surface alloy for Au on Fe(001) might be surprising considering the fact that Au is immiscible in bulk Fe [16]. However, Tersoff showed that surface-confined mixing may generally arise in systems dominated by atomic size mismatch [17] which can explain the present observations (Au atom is 16% larger than the Fe atom).

Figure 2(a) shows the Fe(001) surface after deposition of 0.96 ML Au at 500 K. The growth is certainly not perfectly layer by layer: 0.11 ML of the first layer (marked 1) has been covered with islands (marked 2), while 0.15 ML of the original substrate (marked 0) is still uncovered. An atomically resolved STM image is shown in Fig. 2(b). In addition to the $p(1 \times 1)$ lattice, asymmetric bright features (marked A; 20 pm high) and spherical depressions (marked B; 80 pm deep) are visible. The latter ones have a much lower concentration (1.5% and 0.3% on level 0 and level 1, respectively) and are visible under various tip conditions. Consequently, they are ascribed to impurities. On the contrary, the appearance of the asymmetric features strongly depends on the tip conditions. These features are attributed to intermixed Fe atoms. Their concentration is 6% (2%) on levels 0 and 1 (2). Therefore, adding 0.52 ML Au to the mixed surface layer shown in Fig. 1(b) which contained ~50% Fe results in a surface layer which contains only 6% Fe. Apparently, the Fe concentration in the substrate layer decreased.

To clarify the observations a simple model is sketched in Fig. 3. For simplicity, it is assumed that the surface alloy saturates at exactly 0.5 ML Au [Fig. 3(a)]. The
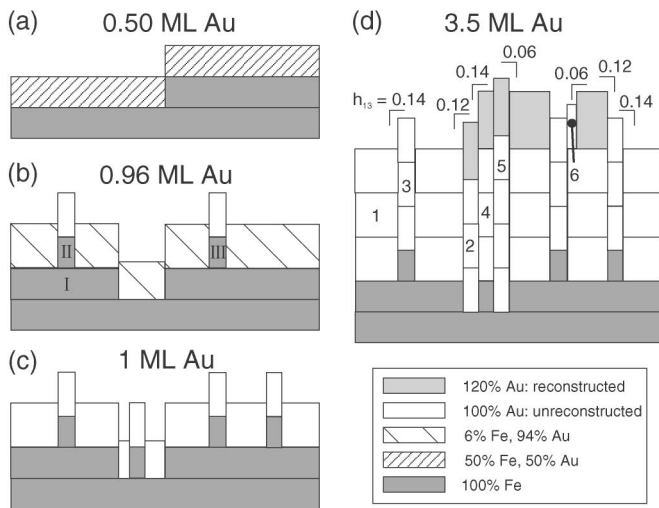
FIG. 3. Schematic model for the alloying-dealloying mechanism leading to interface roughness. (a) Deposition of 0.5 ML Au at 500 K leads to a homogeneous surface alloy. (b) Areas of the alloy which are covered by Au become pure Fe. This Fe is taken out of the alloyed layer which therefore becomes Fe depleted. I, II, and III refer to the explanation in the text. (c) At deposition of ~1 ML all Fe has diffused out of the alloy which has now become a pure Au layer. Since growth of the second Au layer has started before completing the first one, a rough interface is created. (d) Situation after 3.5 ML Au deposition. Fe, Au, and reconstructed surface layers are 0.14, 0.20, and 0.26 nm high, respectively. The reconstructed Au layer contains 20% more Au atoms than the unreconstructed Au layers [18]. The rough interface, the different interlayer spacings of Fe and Au, and the surface reconstruction for Au films thicker than three layers can explain all the levels (numbered) observed in Fig. 4(b).

FIG. 4. STM images of 3.5 ML Au grown on Fe(001) at 500 K. (a) Large scale image (100×100 nm^2, $V_s = -1.0$ V, $I = 0.05$ nA). The surface is rough and partially reconstructed. The circular shapes (see, e.g., two arrows) of the reconstructed layer are obvious. The dotted white arrow indicates the lowest level (marked 0; $h_{01} = 0.14$ nm). (b) Small scale image (50×50 nm^2, $V_s = 1.0$ V, $I = 0.07$ nA). On the lowest unreconstructed level (marked 1), reconstructed (2) and unreconstructed (3) islands are visible. On the reconstructed layer (4), ridges (5) are visible. Small unreconstructed patches (6) which are connected to the reconstructed layer can be observed on level 3. The black circles in (a) show that the ridges are connected to reconstructed patches on the lower terrace. (c) Line profile along the white dotted line in (b). The different height levels indicated in (a), (b), and (c) can be explained by the interface roughness model of Fig. 3.

morphology after deposition of an additional 0.46 ML is shown in Fig. 3(b). According to the experimental results, 0.15 ML of the substrate is uncovered at this stage, while 0.11 ML of the first layer is covered by islands. Therefore, 0.35 ML of the additionally deposited Au covered the alloyed substrate layer. The AuFe alloy is assumed to be surface confined and covering it with Au causes it to demix and to form a pure Fe layer. The Au segregation is probably driven by the large difference in surface energy between Au and Fe and is also reported for studies on Fe/Au(001); see, e.g., [10]. The Fe concentration in the Fe-depleted surface alloy can be calculated if it is realized that 0.46 ML Fe is needed to fill the Au-covered areas denoted I, II, and III in Fig. 3(b). If the Fe in level 2 is neglected (only $0.02 \times 0.11 = 0.002$ ML), the Fe concentration in the uncovered alloyed layer reduces to $(0.5-0.46)/(1-0.11) \times 100\% = 4.5\%$ which is in good agreement with the experimental results [19].

Coverage of more Au will completely deplete the alloy from Fe: at a coverage of ~1 ML [20] the alloy becomes a pure Au layer and Au islands embedded in the original Fe(001) substrate and Fe islands covering the substrate have been created [Fig. 3(c)]. The model shows that this roughened interface is purely a result of the imperfect
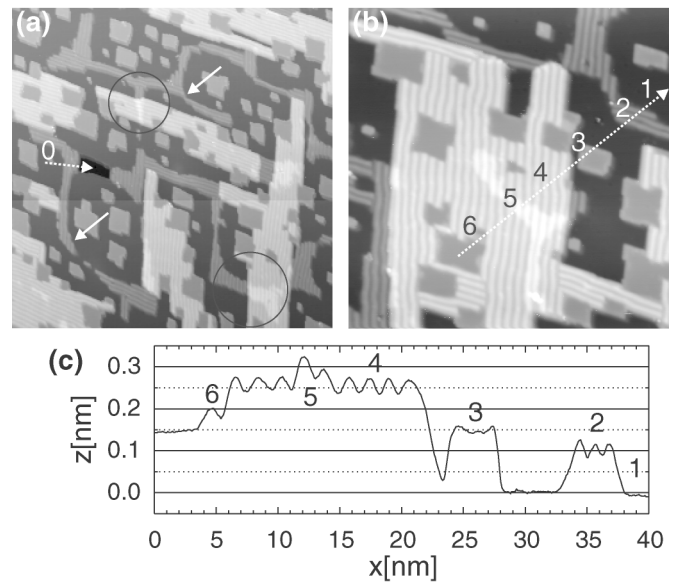
layer-by-layer growth which in turn may be a result of the alloying. If at a deposition of 1 ML the first adlayer had been fully completed without second layer islands, after demixing the first monolayer would be a perfectly flat Au layer. Apparently, the second layer Au islands trap the Fe atoms underneath preventing them from filling the substrate voids.

In contrast to growth at lower temperatures for which perfect layer-by-layer growth is found [21], Fig. 4(a) shows that after deposition of 3.5 ML Au at 500 K a rough surface is obtained. Although various levels can be observed, remarkably all step heights are less than the Au interlayer spacing (0.20 nm). The observation of the characteristic modulation of the quasihexagonal reconstruction on parts of the surface [Fig. 4(b)] implies that these areas are covered by at least 4 ML Au [12]. This reconstruction appears as ridges weakly meandering along the close-packed lattice directions with a periodicity of 1.4 nm [i.e., $(5 \times n)$; see, e.g., [18]] and a corrugation of 0.04 nm. The line profile of Fig. 4(c) shows that relative to the lowest unreconstructed level in Fig. 4(b) (marked 1) the reconstructed islands (2) are 0.12 nm high (h_{12} measured to top of reconstruction), while the

unreconstructed islands (3) are 0.14 nm high (h_{13}). The reconstructed layer (4) is 0.12 nm high compared to level 3 (h_{34}). The height of the ridges (5) on the reconstructed layer (4) is only 0.06 nm relative to level 4 (h_{45}). Finally, small features (6) which are 0.06 nm high relative to level 3 are observed (h_{36}). Although the corrugation of the reconstruction and consequently h_{12} and h_{34} depend on the tunneling conditions [22], such a dependence was not found for h_{13}, h_{45}, and h_{36}.

The reconstructed ridges (5) are connected to the reconstructed islands on the lower terrace (2) forming ringlike patterns as can be seen in Fig. 4(a) (e.g., in areas within black circles). Therefore, it seems likely that these features with heights smaller than the Fe(001) interlayer distance have the same origin. Comparison of Fig. 4(a) with Fig. 2(a) shows that the ringlike patterns resemble the shape of the uncovered substrate patches. Following the model depicted in Fig. 3 describing the results for the submonolayer growth, these patches will turn into Au islands embedded in the Fe substrate upon further deposition. The situation after deposition of 3.5 ML has been sketched in Fig. 3(d). The interface roughness and the surface reconstruction for Au films thicker than three layers can perfectly explain the observed levels. Level 1 consists of three Au layers on top of the original Fe(001) surface. Levels 2 and 5 [and level 0 in Fig. 4(a)] arise from Au islands embedded in the substrate layer [four and five (three) Au layers high, respectively]. Level 3 can be explained by a buried Fe island covered by three Au layers. Level 4 consists of four Au layers (top one reconstructed) on top of the original substrate. Finally, level 6 might be explained by assuming that very small patches of four layer thick Au films are not reconstructed.

From Fig. 3(d) it is clear that h_{25} is the Au step height (0.14 + 0.06 = 0.20 nm), while h_{14} is the height of the reconstructed Au layer (0.12 + 0.14 = 0.26 nm). The latter depends on tunneling conditions [22] which can be explained by electronic effects [9,21]. However, the height differences between unreconstructed layers (i.e., h_{13} and h_{36}) and two reconstructed layers (i.e., h_{45}) do not depend on tunneling conditions which justifies an interpretation of these height differences as geometrical ones caused by interface roughness.

In summary, it was shown that for Au coverages less than 0.5 ML deposited at temperatures above 400 K on Fe(001) a surface alloy is formed. This alloy is stable only at the surface and demixes when it is covered by additional Au. In combination with imperfect layer-by-layer growth conditions, this demixing leads to a rough interface for growth at 500 K. The large difference in interlayer spacing between Fe and Au made it possible to study the buried interface with STM. These results show that the quality of the interface can be controlled and can be studied with high resolution in real space.

*Present address: National Microelectronics Research Centre, University College, Cork, Ireland.
†Present address: Philips Semiconductors, Gerstweg 2, 6534 AE Nijmegen, The Netherlands.
‡Electronic address: hvk@sci.kun.nl

[1] M. N. Baibich et al., Phys. Rev. Lett. **61**, 2472 (1988).
[2] J. S. Moodera et al., Phys. Rev. Lett. **74**, 3273 (1995).
[3] J. Unguris, R. J. Celotta, and D. T. Pierce, Phys. Rev. Lett. **79**, 2734 (1997).
[4] P. Varga and M. Schmid, Appl. Surf. Sci. **141**, 287 (1999).
[5] A. Davies et al., Phys. Rev. Lett. **76**, 4175 (1996).
[6] C. Nagl et al., Phys. Rev. Lett. **75**, 2976 (1995).
[7] P. W. Murray, Phys. Rev. B **55**, 1380 (1997).
[8] S. Heinze et al., Phys. Rev. Lett. **83**, 4808 (1999).
[9] O. S. Hernan et al., Surf. Sci. **415**, 106 (1998).
[10] V. Blum et al., Phys. Rev. B **59**, 15 966 (1999).
[11] N. Spiridis and J. Korecki, Appl. Surf. Sci. **141**, 313 (1999).
[12] J. Unguris, R. J. Celotta, and D. T. Pierce, J. Appl. Phys. **75**, 6437 (1994).
[13] J. Opitz et al., Phys. Rev. B **63**, 094418 (2001).
[14] G. de Raad, P. Koenraad, and J. H. Wolter, J. Vac. Sci. Technol. B **17**, 1946 (1999).
[15] J. A. Stroscio et al., Phys. Rev. Lett. **75**, 2960 (1995).
[16] A. R. Miedema, P. F. de Chatel, and F. R. de Boer, Physica (Amsterdam) **100B**, 1 (1980).
[17] J. Tersoff, Phys. Rev. Lett. **74**, 434 (1995).
[18] X. Gao, A. Hamelin, and M. J. Weaver, Phys. Rev. B **46**, 7096 (1992).
[19] The uncertainties in the experimentally obtained concentrations and coverages are estimated to be ±1%.
[20] The exact coverage depends on the details of the processes involved.
[21] R. G. P. van der Kraan, Ph.D. thesis, University of Nijmegen, 1995; M. M. J. Bischoff et al. (to be published).
[22] For example, at $V_s = -0.5$ V and $I = 0.5$ nA the "hex" corrugation reduced to ~0.01 nm and consequently h_{12} (h_{14}) to 0.09 nm (0.23 nm).